Journal of Coordination Chemistry

ISSN: 0095-8972 (Print) 1029-0389 (Online) Journal homepage: http://www.tandfonline.com/loi/gcoo20

Synthesis and structure of a 1-D copper(II) coordination polymer bridged both by oxamido and carboxylate: in vitro anticancer activity and reactivity toward DNA and protein BSA

Xue-Jie Li, Kang Zheng, Yan-Tuan Li, Cui-Wei Yan, Zhi-Yong Wu & Shi-Ying Xuan

To cite this article: Xue-Jie Li, Kang Zheng, Yan-Tuan Li, Cui-Wei Yan, Zhi-Yong Wu & Shi-Ying Xuan (2015) Synthesis and structure of a 1-D copper(II) coordination polymer bridged both by oxamido and carboxylate: in vitro anticancer activity and reactivity toward DNA and protein BSA, Journal of Coordination Chemistry, 68:5, 928-948, DOI: 10.1080/00958972.2015.1009452

To link to this article: http://dx.doi.org/10.1080/00958972.2015.1009452

Journal of Coordination Chemistry, 2015
Vol. 68, No. 5, 928–948, http://dx.doi.org/10.1080/00958972.2015.1009452

Synthesis and structure of a 1-D copper(II) coordination polymer bridged both by oxamido and carboxylate: *in vitro* anticancer activity and reactivity toward DNA and protein BSA

XUE-JIE LI†, KANG ZHENG†, YAN-TUAN LI*†, CUI-WEI YAN‡, ZHI-YONG WU† and SHI-YING XUAN*§

†Marine Drug & Food Institute, Ocean University of China, Qingdao, PR China
‡College of Marine Life Science, Ocean University of China, Qingdao, PR China
§Qingdao Municipal Medical Group, Qingdao, PR China

(*Received 24 June 2014; accepted 21 November 2014*)

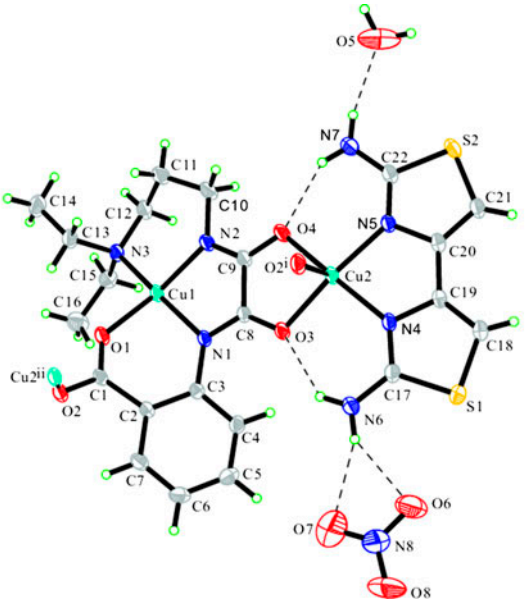

A new 1-D copper(II) coordination polymer was synthesized and structurally characterized. *In vitro* anticancer activity and reactivity toward DNA and protein of the copper(II) polymer was studied.

A 1-D copper(II) coordination polymer formulated as $\{[Cu_2(bdpox)(dabt)](NO_3)\cdot H_2O\}_n$, where H_3bdpox and dabt denote *N*-benzoate-*N*′-[3-(diethylamino)propyl]oxamide and 2,2′-diamino-4,4′-bithiazole, respectively, was synthesized and characterized by elemental analyses, molar conductance

*Corresponding authors. Email: yantuanli@ouc.edu.cn (Y.-T. Li); xuansy619@163.com (S.-Y. Xuan)

measurement, IR and electronic spectra studies, and single-crystal X-ray diffraction. The crystal structure analysis reveals that copper(II) ions are bridged by both *cis*-oxamido and carboxylato groups to form a 1-D coordination polymer with corresponding Cu···Cu separations of 5.2420(10) and 5.1551(8) Å. The *endo*- and *exo*-copper(II) ions of the *cis*-oxamido-bridge are located in distorted square-planar and square-pyramidal geometries, respectively. There is a 2-D hydrogen bonding network in the crystal. The *in vitro* anticancer activities suggest that the copper(II) complex is active against selected tumor cell lines. The reactivities toward herring sperm DNA and bovine serum albumin (BSA) reveal that the copper(II) complex can interact with DNA by intercalation and effectively quench the intrinsic fluorescence of BSA via a static mechanism. The influence of hydrophobicity of the substituents in bridging ligands on DNA and protein binding properties and the *in vitro* anticancer activities of such copper(II) polymers is discussed.

Keywords: 1-D Copper(II) coordination polymer; μ-Oxamidato-bridge; μ-Carboxylate-bridge crystal structure; DNA-binding; Protein BSA interaction; *In vitro* anticancer activity

1. Introduction

The design and synthesis of transition metal complexes that can interact with DNA and protein by noncovalent modes have attracted interest in the field of metallo-pharmaceuticals. Interest in this area stems from the facts that DNA and protein are commonly considered as the main molecular targets in the action of drugs, and many metal complexes exert their drug effects through binding to DNA or protein, which is the basis for designing and discovering new and more efficient metal-based antitumor drugs [1–6]. Thus, the reactivity toward DNA and protein of metal complexes are a fundamental requirement, not only for the relevant theoretical interest to elucidate the mechanism involved in site-specific recognition of DNA, and the biochemical procedures governing protein sequencing, but also for application of probes of DNA structure, and the exploitation of the rational design and synthesis of new types of pharmaceutical molecules.

In the context of design and synthesis of metal complexes that are capable of binding DNA and protein by noncovalent modes, most attention has centered upon selection of metal ions and design of ligands. Metal complexes can accelerate drug action and increase effectiveness of organic ligands [7], and medicinal properties of metal complexes depend on the nature of metal ions and ligands. Thus, a combination of suitable metal as well as ligand is important for construction of a highly efficient DNA and bovine serum albumin (BSA) targeted drug. A number of copper(II) complexes with different ligands have been widely studied [8–11], because copper, as a biologically active metal, has many correlations with endogenous oxidative deoxyribonucleic acid damage associated with aging and cancer. Furthermore, significant developments have occurred in recent years in the chemistry of polymer–metal complexes, particularly in the study of interaction of polymer–metal complexes with DNA [12, 13]. These polymer–metal complexes act as excellent models for metalloenzymes, lead to the development of highly efficient catalysts [14, 15], and as potential candidates for selective delivery of anticancer agents to tumor tissue [16]. However, examples of such polymer–metal complexes are still few, and comparatively little attention has been given to the studies of interactions with DNA and proteins. This prompted us to synthesize and study new polymer–metal complexes to gain some insight into their DNA/protein binding property and antitumor activities.

In view of the bioactivities of copper(II) complexes with 2,2′-diamino-4,4′-bithiazole (dabt) and its derivatives [17–19], and the effective bridging function of oxamide groups, we reported the synthesis, structure, and DNA-binding of two 1-D copper(II) polymers with

asymmetric *N*,*N*′-bis(substituted)oxamide as bridging ligands and dabt as coligands [20, 21]. In order to understand the influence of the various bridging ligands in polymeric copper(II) complexes on structure, DNA- and BSA-binding properties as well as cytotoxic activities, and to gain insight into the structure–activity relationship of this kind of polymeric copper(II) complex, in this article, we used *N*-benzoate-*N*′-[3-(diethylamino)propyl] oxamide (H_3bdpox) as bridging ligand and dabt as coligand to synthesize and structurally characterize a new 1-D polymeric copper(II) complex, $\{[Cu_2(bdpox)(dabt)](NO_3)\cdot H_2O\}_n$. *In vitro* cytotoxic activity and the reactivity toward DNA and protein BSA of the polymeric copper(II) complex were studied. The main results of the present investigation confirmed that hydrophobicity of different substituent groups on bridging ligands in these polymeric copper(II) complex systems can influence DNA-binding and the *in vitro* anticancer activity, thus suggesting that the DNA-binding ability and the anticancer activity may be tuned through differences of the bridge ligands in these polymer–copper(II) systems, which are useful for the synthesis of new metal-based drugs targeting DNA.

2. Experimental

2.1. *Materials and chemicals*

All reagents were of AR grade and obtained commercially. *N*-benzoate-*N*′-[3(diethylamino) propyl]oxamide (H_3bdpox) was synthesized according to literature method [22]. Herring sperm DNA (*HS*-DNA), Ethidium bromide (EB), and BSA were purchased from Sigma Corp. and used as supplied.

2.2. *Physical measurements*

The C, H, and N elemental analyses were performed with a 240-Perkin-Elmer elemental analyzer. Molar conductance was measured with a Shanghai DDS-11A conductometer. The infrared spectrum was recorded with samples as KBr pellets in a Nicolet-470 spectrophotometer from 4000 to 400 cm^{-1}. The UV–vis spectrum was recorded in a 1 cm path length quartz cell on a Cary 300 spectrophotometer. Fluorescence was tested on an Fp-750w fluorometer. A CHI 832 electrochemical analyzer (Shanghai CHI Instrument, Shanghai, China) in connection with a glassy carbon working electrode (GCE), a saturated calomel reference electrode, and a platinum wire counter electrode was used for electrochemical measurements. The GCE surface was freshly polished to a mirror prior to each experiment with 0.05 μm α-Al_2O_3 paste and then cleaned in water for 5 min. Viscosity measurement was carried out using an Ubbelohde viscometer immersed in a thermostatic water bath maintained at 298 K.

2.3. *Synthesis of* $\{[Cu_2(bdpox)(dabt)](NO_3)\cdot H_2O\}_n$

To a stirred ethanol solution (10 mL) of H_3bdpox (0.0151 g, 0.05 mM) and piperidine (0.0128 g, 0.15 mM), an ethanol solution (5 mL) containing $Cu(NO_3)_2\cdot 3H_2O$ (0.0242 g, 0.1 mM) was added dropwise at room temperature. The mixture was stirred quickly for 30 min and an ethanol solution (5 mL) of dabt (0.0099 g, 0.05 mM) was added. The reaction solution was heated at 333 K with stirring for 6 h and then cooled to room

temperature. The resulting dark green solution was filtered and dark brown cube crystals of the polymeric copper(II) complex suitable for X-ray analysis were obtained by slow evaporation at room temperature after 15 days. Yield: 0.0296 g (82%). Anal. Calcd for $Cu_2C_{22}H_{28}N_8O_8S_2$ (%): C, 36.51; H, 3.90; N, 15.48. Found (%): C, 36.62; H, 3.97; N, 15.32. Λ_M (DMF solution): 78 S·cm^2 M^{-1}.

2.4. *X-ray structure determination*

The X-ray diffraction experiments were made on a Bruker APEX area-detector diffractometer with graphite monochromated Mo Kα radiation (λ = 0.71073 Å) at 296 K. The crystal structure was solved by the directed method followed by Fourier syntheses. Structure refinements were performed by full matrix least-squares procedures using SHELXL-97 on F^2 [23]. The hydrogens on dabt and water were found in a difference Fourier map. Then the water hydrogens were treated as riding with restrained H–O distances (0.86 Å). The hydrogens on C and N of dabt were refined freely except restrained H–N bond lengths of N6 (0.86 Å). The remaining hydrogens were placed in calculated positions, with C–H = 0.96 (methyl), 0.97 (methylene), and 0.93 Å (aromatic), then refined in riding mode, with U_{iso}(H) = 1.5 (methyl) or 1.2U_{eq} (carrier atoms). Crystal data and structural refinement parameters are summarized in table 1 and selected bond distances and angles are listed in table 2.

2.5. In vitro *cytotoxic activity evaluation by SRB assays*

In vitro cytotoxic activities of the polymeric copper(II) complex together with *cis*-platin were evaluated against selected cell lines by using the sulforhodamine B (SRB) assays. All

Table 1. Crystal data for {[Cu_2(bdpox)(dabt)] $NO_3 \cdot H_2O$}$_n$.

Formula	$C_{22}H_{28}Cu_2N_8O_8S_2$
Formula weight	723.76
Crystal system	Orthorhombic
Space group	Pbca
a (Å)	14.119(3)
b (Å)	15.077(3)
c (Å)	26.539(6)
α (°)	90
β (°)	90
γ (°)	90
V (Å^3)	5649(2)
Z	8
D(Calcd) [g cm^{-3}]	1.702
μ (Mo Kα) (mm^{-1})	1.715
F(0 0 0)	2960
Crystal size [mm]	0.13 × 0.18 × 0.22
Temperature (K)	296
Radiation [Å]	Mo Kα 0.71073
θ range	2.1–27.5
Tot., Uniq. Data, R(int)	31,269, 6508, 0.052
Observed data [$I > 2\sigma(I)$]	4450
R, ωR_2, S	0.0364, 0.0900, 1.01
Max. and Av. shift/error	0.00, 0.00

Table 2. Selected bond distances (Å) and angles (°) for **1**.

Bond distances (Å)			
Cu1–O1	1.9174(19)	Cu1–N1	1.990(2)
Cu1–N2	1.960(2)	Cu1–N3	2.058(2)
Cu2–O3	1.9762(19)	Cu2–O4	1.9552(19)
Cu2–N4	1.977(2)	Cu2–N5	1.979(2)
Cu2–O2^{i}	2.309(2)	O1–C1	1.278(3)
Bond angles (°)			
O1–Cu1–N1	90.54(8)	O1–Cu1–N2	154.26(10)
O1–Cu1–N3	93.60(8)	N1–Cu1–N2	83.99(9)
N1–Cu1–N3	168.95(10)	N2–Cu1–N3	96.50(9)
O3–Cu2–O4	83.87(8)	O3–Cu2–N4	95.47(8)
O3–Cu2–N5	166.91(9)	O3–Cu2–O2^{i}	91.99(7)
O4–Cu2–N4	169.05(10)	O4–Cu2–N5	169.3(2)
O4–Cu2–O2^{i}	98.23(17)	N4–Cu2–N5	95.42(9)
N4–Cu2–O2^{i}	97.80(8)	N5–Cu2–O2^{i}	101.05(8)
Cu1–O1–C1	129.85(17)	Cu1–N3–C15	112.66(18)
Cu2–O4–C9	112.22(17)		

Note: Symmetry code: (i) $-1/2 + x$, $1/2 - y$, $1 - z$.

cells were cultured in RPMI 1640 supplemented with 10% (v/v) fetal bovine serum, 1% (w/v) penicillin (104 U mL^{-1}), and 10 mg mL^{-1} streptomycin. Cell lines are maintained at 310 K in a 5% (v/v) CO_2 atmosphere with 95% (v/v) humidity. Cultures were passaged weekly using trypsine-EDTA to detach the cells from their culture flasks. The polymeric copper(II) complex was dissolved in DMSO and diluted to the required concentration with culture medium when used. The content of DMSO in the final concentrations did not exceed 0.1%. At this concentration, DMSO was non-toxic to the cells tested. Rapidly growing cells were harvested, counted, and incubated at the appropriate concentration in 96-well microplates for 24 h. The polymeric copper(II) complex dissolved in culture medium was then applied to the culture wells to achieve final concentrations from 10^{-4} to 10^{-1} μM. Control wells were prepared by addition of culture medium without cells. The plates were incubated at 310 K in a 5% CO_2 atmosphere for 48 h. Upon completion of the incubation, the cells were fixed with ice-cold 10% trichloroacetic acid (100 mL) for 1 h at 277 K, washed five times in distilled water, and allowed to dry in the air and stained with 0.4% SRB in 1% acetic acid (100 mL) for 15 min. The cells were washed four times in 1% acetic acid and air-dried. The stain was solubilized in 10 mM unbuffered Tris base (100 mL) and the OD of each well was measured at 540 nm on a microplate spectrophotometer. The IC_{50} value was calculated from the curve constructed by plotting cell survival (%) *versus* the polymeric copper(II) complex concentration.

2.6. *DNA-binding experiments*

All experiments involving *HS*-DNA were performed in Tris–HCl buffer solution (pH 7.14), which was prepared using deionized and sonicated triple distilled water. Solution of DNA in Tris–HCl buffer gave the ratio of UV absorbance at 260 and 280 nm, A_{260}/A_{280}, of *ca.*1.9, indicating that the DNA was sufficiently free of protein [24]. The concentration of the DNA stock solution was determined according to its absorbance at 260 nm. The molar absorption coefficient, ε_{260}, was taken as 6600 M^{-1} cm^{-1} [25]. Stock solution of DNA was stored at 277 K and used after no more than four days. Concentrated stock solution of the polymeric copper(II) complex was prepared by dissolving the polymeric copper(II) complex

in DMSO and diluting suitably with Tris–HCl buffer to required concentrations for all the experiments. Absorption spectral titration experiments were performed by keeping the concentration of the polymeric copper(II) complex constant while varying *HS*-DNA concentration. Equal solution of *HS*-DNA was added to the polymeric copper(II) complex solution and reference solution to eliminate the absorbance of *HS*-DNA itself. In the EB fluorescence displacement experiment, 5 μL of the EB Tris–HCl solution (1 mM) was added to 1 mL of *HS*-DNA solution (at saturated binding levels) [26] and stored in the dark for 2 h. Then, the solution of the polymeric copper(II) complex was titrated into the DNA/EB mixture and diluted in Tris–HCl buffer to 5 mL. Before measurements, the mixture was shaken and incubated at room temperature for 30 min. The fluorescence spectra of EB bound to *HS*-DNA were obtained at an emission wavelength of 584 nm in the fluorometer. In viscosity measurement, *HS*-DNA sample approximately 200 base pairs in length was prepared by sonication in order to minimize complexities arising from DNA flexibility [27]. Flow times were measured with a digital stopwatch, each sample was measured three times, and an average flow time was calculated. Relative viscosities for *HS*-DNA in the presence and absence of the polymeric copper(II) complex were calculated from the relation $\eta = (t - t_0)/t_0$, where t is the observed flow time of DNA-containing solution and t_0 is that of Tris–HCl buffer alone. Data were presented as $(\eta/\eta_0)^{1/3}$*versus* binding ratio [28], where η is the viscosity of DNA in the presence of the polymeric copper(II) complex and η_0 is the viscosity of DNA alone.

2.7. *BSA interaction experiments*

All experiments involving BSA were performed in 50 mM NaCl/Tris–HCl buffer solution (pH 7.14). Solutions of BSA protein and the polymeric copper(II) complex were prepared by dissolving them in the NaCl/Tris–HCl buffer solution to required concentrations. For UV absorption experiment, a 5 mL solution of BSA (10 μM) was titrated with various concentrations of the polymeric copper(II) complex. Equal solutions of the polymer were added to the reference solutions to eliminate the absorbance of the polymeric copper(II) complex itself. In the tryptophan fluorescence quenching experiment, quenching of the tryptophan residues of BSA [29] was done by keeping the concentration of the BSA constant while varying the polymeric copper(II) complex concentration, producing solutions with varied mole ratio of the quenchers to BSA. Titrations were manually done using a micropipette for addition of the polymeric copper(II) complex. The fluorescence spectra were recorded at an excitation wavelength of 295 nm and an emission wavelength of 347 nm in the fluorometer after each addition of quencher.

3. Results and discussion

3.1. *Synthetic route and general properties of the polymeric copper(II) complex*

In order to obtain polymeric copper(II) complex bridged by asymmetric *N*,*N*′-bis(substituted)-oxamide, *N*-benzoate-*N*′-[3-(diethylamino)propyl]oxamide (H_3bdpox), which can coordinate to metal ions through carbonyl oxygens and nitrogens of oxamido as well as oxygens of carboxyl [22], was chosen as bridging ligand. Simultaneously, 2,2′-diamino-4,4′-bithiazole (dabt) was used as coligand. In preparing the polymeric copper(II) complex,

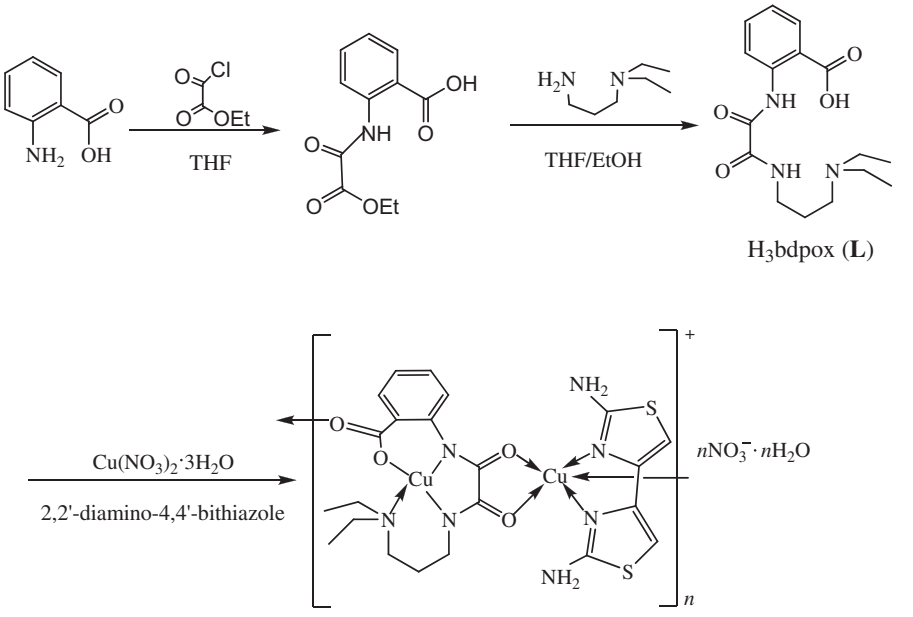

Scheme 1. The synthetic pathway for bridging H_3bdpox (L) and its copper(II) polymer.

the use of piperidine as base makes the bridging ligand (H_3bdpox) coordinate to copper(II) through the deprotonated oxamido nitrogen and carboxyl oxygens. Elemental analyses indicate that the reaction of H_3bdpox with $Cu(NO_3)_2{\cdot}3H_2O$ and dabt in 1 : 2 : 1 M ratio yielded the new 1-D copper(II) coordination polymer, $\{[Cu_2(bdpox)(dabt)](NO_3){\cdot}H_2O\}_n$. The synthetic pathway for the H_3bdpox and its copper(II) polymer may be represented by scheme 1.

The polymeric copper(II) complex is insoluble in non-polar solvents and common polar solvents, and very soluble in DMF and DMSO to give stable solutions at room temperature. In the solid state, the copper(II) coordination polymer is fairly stable in air so as to allow physical measurements.

3.2. *IR spectra*

IR spectrum from 4000 to 400 cm^{-1} provides some information regarding the mode of coordination in the polymeric copper(II) complex and is analyzed in a careful comparison with that of free H_3bdpox. The antisymmetric stretching vibration of the carboxylate $\nu_{as(COO)}$, together with the carbonyl stretching vibration of oxamidate group $\nu_{(C=O)}$ at 1684 cm^{-1} of the bridging ligand H_3bdpox are considerably shifted to lower frequency of 1644 cm^{-1} in the IR spectrum of the polymer–copper(II), implying that the carbonyl oxygens of oxamido and oxygens of carboxylate bridge copper(II) ions form the coordination polymer [30]. This shift has often been used as a diagnostic for oxamido-bridged structures [22]. The $\nu_{(C=N)}$ stretch of the aromatic ring of dabt was found at 1577–1526 cm^{-1}, indicating that the nitrogen of dabt are coordinated to copper(II) ions in the copper(II) polymer. Furthermore, bands at 1384–1336 cm^{-1}, typical for the ionic nitrate [30], were also observed for the polymeric copper(II) complex.

3.3. *Electronic spectra*

To obtain further structural information, the electronic spectrum of the polymeric copper(II) complex was measured. For the polymeric copper(II) complex, two main absorptions with varied intensities can be observed. The intense band at 233 nm is assignable to inter- or intra-ligand (π–π*) transition, while the band at 274 nm in the polymeric copper(II) complex can be assigned to the charge transfer transition between the ligand and metal [31].

These spectroscopic data of the polymeric copper(II) complex are further supported by the determination of the crystal structure (*vide infra*).

3.4. *Structure description of {[Cu_2(bdpox)(dabt)](NO$_3$)·H_2O}$_n$*

As shown in figure 1, the asymmetric unit of the copper(II) coordination polymer {[Cu_2(bdpox)(dabt)](NO$_3$)·H_2O}$_n$ is a bicopper(II) complex cation with a bridging *cis*-bdpox^{3-} ligand and a dabt coligand, with a nitrate ion and a solvent water molecule. These asymmetric units bond end-to-end through the carboxyl bridges to form a 1-D coordination polymeric chain extending along the *a*-axis. The two copper(II) ions, Cu1 and Cu2, are in a distorted {N_3O} square-planar and {N_2O_3} square-pyramidal coordination geometries,

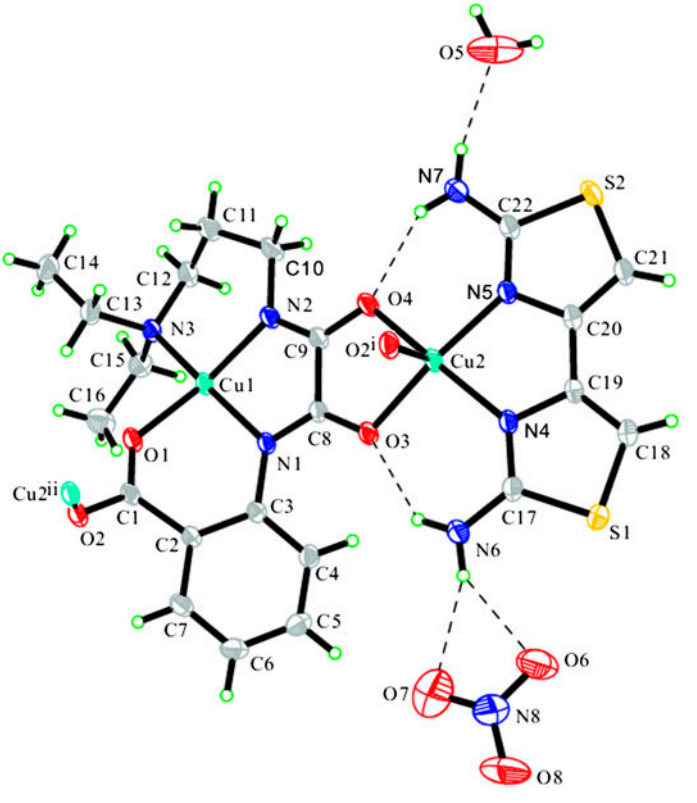

Figure 1. A view of **1** with the atomic numbering scheme. Displacement ellipsoids are drawn at the 30% probability level and hydrogens are shown as small spheres of arbitrary radii. Dashed lines indicate hydrogen bonds [symmetry codes: (i) $-1/2 + x$, $1/2 - y$, $1 - z$; (ii) $1/2 + x$, $1/2 - y$, $1 - z$].

Table 3. Hydrogen-bonding geometries (Å, °) for **1**.

D–H···A	*D*–H	H···A	*D*···A	*D*–H···A
N6–H6A···O3	0.85(2)	2.19(3)	2.889(3)	140(2)
N6–H6B···O6	0.850(19)	2.31(2)	3.045(5)	146(3)
N6–H6B···O7	0.850(19)	2.33(2)	3.135(6)	158(3)
N7–H7A···O4	0.83(4)	2.15(4)	2.890(4)	148(3)
N7–H7B··· O5	0.83(4)	2.09(4)	2.898(6)	165(4)
C15–H15A···S1^{iii}	0.97	2.85	3.549(3)	129

Note: Symmetry code: (iii) $1-x, -y, 1-z$.

respectively. The coordination distortion of Cu1 is very obvious, O1 deviates 0.1928(17) Å off the plane of N1–N3. The tetrahedral volume of $\{N_3O\}$ is 1.528 Å^3. Cu2 has a square-pyramidal τ value of 0.04 [32] and is displaced from the basal plane 0.2064(12) Å with axial Cu2–O2^i distance of 2.308(2) Å [table 2, symmetry code: (i) $x-1/2, 1/2-y, 1-z$]. The Cu···Cu distances through the *cis*-oxamido and the carboxyl bridges are 5.2420(10) and 5.1551(8) Å, respectively. The bite angles of the oxamide-bridge at Cu1 and Cu2 are 83.98(9)° and 83.87(8)°, respectively. The torsion angles, Cu1–O1–C1–O2 [154.5(2)°] and Cu2^{ii}–O2–C1–O1 [−99.6(3)°, symmetry code: (ii) $x+1/2, 1/2-y, 1-z$], indicate a carboxylato-bridge in nonplanar skew–skew fashion [33, 34].

All seven N and O atoms of the bdpox^{3-} ligand take part in coordination to copper(II) ions forming four chelate rings. Two five-membered rings are planar, whereas the two six-membered rings are puckered. Cu1–O1–C1–C2–C3–N1 ring is a compressed boat conformation with puckering parameters [35] of Q [0.344(2) Å], θ [85.1(3)°] and φ [309.9(4)°]. N1 and C1 displace out of the boat bottom 0.332(3) and 0.253(4) Å, respectively. While

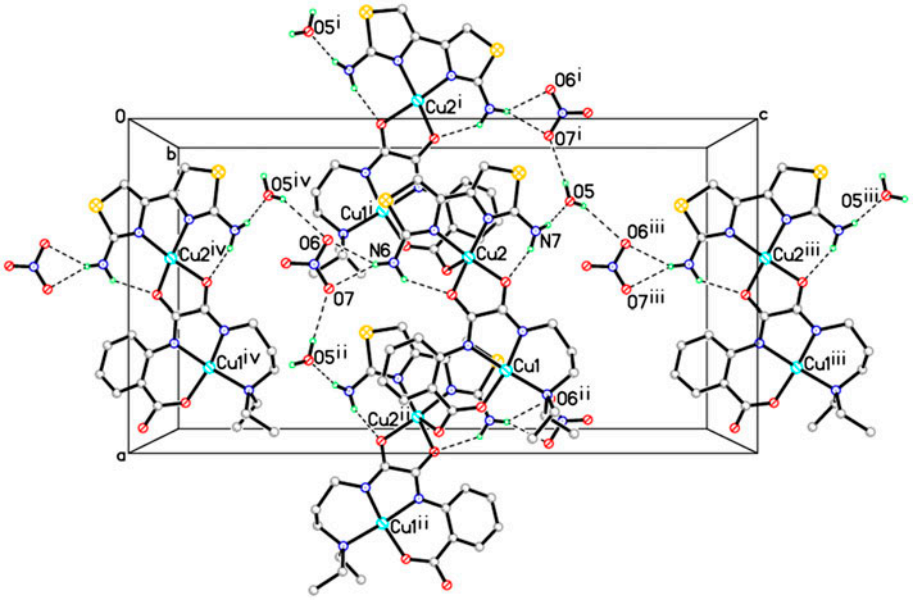

Figure 2. A 2-D hydrogen bonding network parallel to the plane (0 1 0). Symmetry codes: (i) $x-1/2, -y+1/2, -z+1$; (ii) $x+1/2, -y+1/2, -z+1$; (iii) $x, -y+1/2, z+1/2$; (iv) $x, -y+1/2, z-1/2$.

Cu1–N2–C10–C11–C12–N3 ring is close to a half-chair, the parameters are Q [0.584(3) Å], θ [60.3(3)°], and φ [212.9(3)°]. The Cu1–N3 bond [2.058(2) Å] is longer than Cu1–N1 [1.990(2) Å] and Cu1–N2 [1.960(2) Å], consistent with stronger donor ability of the deprotonated amido nitrogen compared with the amino nitrogen [36].

Hydrogen bonding (table 3) and π–π stacking interactions play important roles in construction of the supermolecule in the crystal. As shown in figure 2, there is a hydrogen bonding chain formed by nitrate ions and solvent water molecules parallel to the *a*-axis, *viz.* parallel to the complex chain. Furthermore, these two kinds of chains link to build up a 2-D network parallel to *a0c* plane. As viewed from figure 3, an offset π–π stacking interaction is observed between the benzene ring of a $bdpox^{3-}$ ligand and the S1-thiazole ring of another $bdpox^{3-}$ ligand at $1-x, -y, 1-z$ (v), and *vice versa*. They have a dihedral angle of 13.27 (14)° and a center-to-center distance of 3.6895(19) Å. The angles of their center-to-center vector with the normals to the benzene ring and thiazole ring are 21.33° and 21.23°, respectively.

Comparing $\{[Cu_2(bdpox)(dabt)](NO_3)\cdot H_2O\}_n$ with our previously reported copper(II) polymers $\{[Cu_2(dmaepox)(dabt)](pic)\cdot H_2O\}_n$ [20] and $\{[Cu_2(dmaepob)(dabt)](NO_3)\cdot 0.6H_2O\}_n$ [21], where H_3dmaepox and H_3dmapob stand for *N*-(2-carboxylatophenyl)-*N*′-[3-(methylamino)-propyl]oxamidate and *N*-(2-carboxylatophenyl)-*N*′-[3-(dimethylamino)propyl]oxamidate, respectively, the three copper(II) polymers have the same coligand (dabt) and metal ions (Cu^{2+}), with the bridging ligands skeleton also being similar.

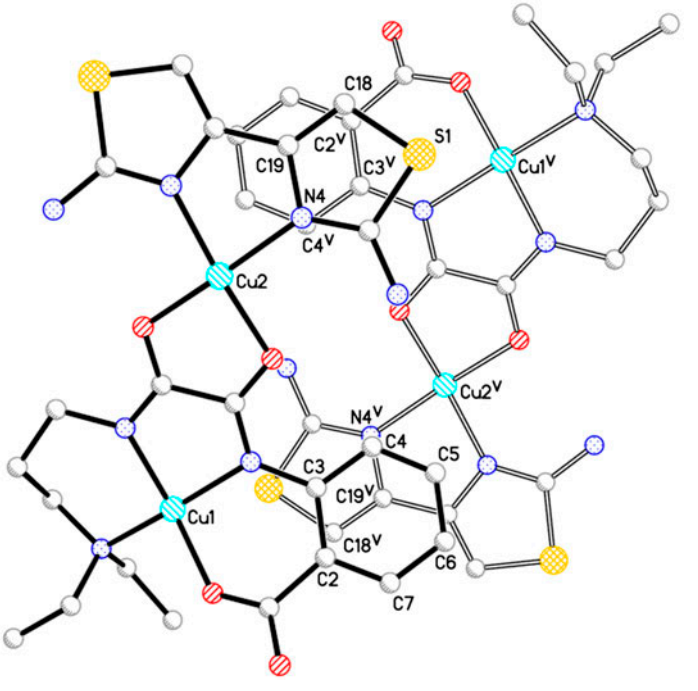

Figure 3. A perspective view along the normal to the benzene ring (C2–C7) of an offset π–π stacking interaction existing among the hydrogen bonding layers above. The separations of eclipsed atoms to the opposite aromatic rings are 3.729(4) ($C2^{v}$), 3.466(3) ($C3^{v}$), 3.692(4) ($C18^{v}$), and 3.425(3) Å ($C19^{v}$). Symmetry code: (v) $1-x, -y, 1-z$.

The main difference is the substituents on nitrogen of the primary amino group, which resulted in the present copper(II) polymer $\{[Cu_2(bdpox)(dabt)](NO_3)\cdot H_2O\}_n$ crystallizing in orthorhombic with *Pbca* space group, while the previously reported copper(II) coordination polymers $\{[Cu_2(dmaepox)(dabt)](pic)\cdot H_2O\}_n$ and $\{[Cu_2(dmaepob)(dabt)](NO_3)\cdot 0.6H_2O\}_n$ were monoclinic with $P2_1/c$ space group. These dissimilarities resulted in distinct structure and further affect DNA/BSA binding properties and *in vitro* anticancer activities.

The present polymeric copper(II) complex in the solid state may be a discrete binuclear species in solutions, although the molar conductance value of the polymeric copper(II) complex (78 S cm^2 (M^{-1}) in DMF solution falls in the expected range for a 1 : 1 electrolyte [37], and the electric spectra obtained for the polymeric copper(II) complex at different concentrations (7.2×10^{-5} to 7.2×10^{-7} M) obeyed the Beer–Lambert law. Indeed, it is difficult to determine whether the polymer–copper(II) stays intact in solutions as the 1-D coordination polymer in the crystal structure, since the possibility of the polymeric copper (II) complex falling apart in solutions cannot be excluded. Therefore, it would be more reasonable to name the compound as **1** and replace the wording "coordination polymer" with "complex **1**" in the following biological activity studies.

3.5. *DNA interaction studies*

DNA is the primary target for many metal-based drugs, and many metal complexes exert their drug effects through binding to DNA. Understanding the features that determine the binding of metal complexes to DNA would be valuable in the rational design of sequence-specific DNA binding molecules for application in chemotherapy and in the development of tools for biotechnology. As a result, the elucidation of noncovalent interactions with DNA by **1** was explored with the aid of different techniques and methods.

3.5.1. Electronic absorption titration. Electronic absorption spectroscopy is an effective method to examine the binding mode and magnitude of DNA with metal complexes. In general, hypochromism and red-shift are associated with the binding of the metal complexes to the DNA helix, due to intercalative mode involving a strong stacking interaction between the aromatic chromophore of metal complexes and the base pairs of DNA [38]. The absorption spectra of **1** in the absence and presence of *HS*-DNA are depicted in figure 4. In the presence of incremental amounts of *HS*-DNA, a significant hypochromic effect accompanied the moderate bathochromic shift (4 nm) of the absorbance maximum at 233 nm for the copper(II) complex. Obviously, these spectral characteristics reveal that **1** can interact with *HS*-DNA basically through the intercalation because intercalation would lead to hypochromism and bathochromism in UV absorption spectra on account of the intercalative mode involving a strong interaction between the aromatic chromophore and the base pairs of the DNA [39]. These observations for **1** can be confirmed by the following. When **1** intercalates the base pairs of *HS*-DNA, the π^*-orbital of the intercalated ligand in **1** can couple with the π-orbital of the base pairs, thus decreasing the π–π^* transition energy and resulting in bathochromism. Furthermore, the coupling π^*-orbital is partially filled by electrons, thereby decreasing the transition probabilities and concomitantly resulting in hypochromism.

In order to quantitatively evaluate the strength of the binding affinity of **1** toward *HS*-DNA, the intrinsic binding constant K_b of **1** with *HS*-DNA was determined by monitoring the changes in absorbance at 233 nm with increasing concentration of *HS*-DNA according to the following equation [40]:

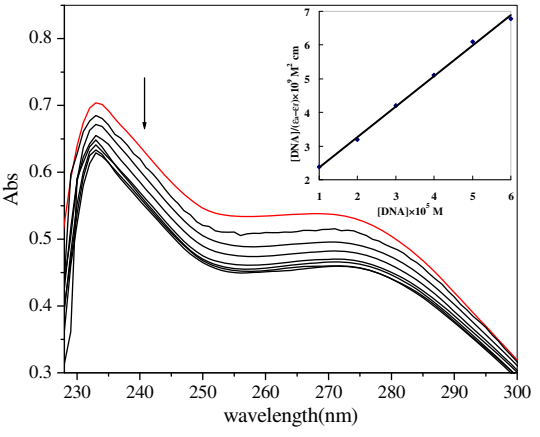

Figure 4. Absorption spectra of **1** upon titration of *HS*-DNA. Arrow indicates the change upon increasing the DNA concentration. Inset: plot of $[DNA]/(\varepsilon_a - \varepsilon_f)$ *vs.* [DNA] for the absorption titration of *HS*-DNA with **1**.

$$[DNA]/(\varepsilon_a - \varepsilon_f) = [DNA]/(\varepsilon_b - \varepsilon_f) + 1/K_b(\varepsilon_b - \varepsilon_f) \quad (1)$$

where [DNA] is the concentration of DNA, ε_f, ε_a, and ε_b correspond to the extinction coefficient, respectively, for free **1**, for each addition of DNA to their solutions and for **1** in the fully bound form. From the $[DNA]/(\varepsilon_a - \varepsilon_f)$ *versus* [DNA] plot (inset in figure 4), the K_b value for **1** was estimated to be $6.16 \times 10^4\ M^{-1}$ ($R = 0.9989$ for six points), lower than that of a classical intercalator, such as EB-DNA [41], but higher than those of some bi- [42–44] and tetracopper(II) complexes [45], and has the same level as those of well-established intercalation agents [46], indicating that **1** strongly binds to *HS*-DNA, and this may be related to structural characteristics.

Comparing the K_b value of **1** (K_b, $6.16 \times 10^4\ M^{-1}$) with those of our previously reported analogous polymeric copper(II) complexes $\{[Cu_2(dmaepox)(dabt)](pic)\cdot H_2O\}_n$ (K_b, $1.25 \times 10^4\ M^{-1}$) and $\{[Cu_2(dmapob)(dabt)](NO_3)\cdot 0.6H_2O\}_n$ (K_b, $1.04 \times 10^4\ M^{-1}$) [20], the K_b value of **1** is higher than those of the previously reported polymeric copper(II) complexes, indicating that **1** strongly binds to *HS*-DNA by intercalation. The main difference among the three copper(II) compounds is that the substituents of nitrogen of the primary amino group on the bridging ligands are one methyl group (H_3dmaepox), two methyl groups (H_3dmapob), and two ethyl groups (H_3bdpox), respectively, which would be expected to hinder intercalation of **1**, and hence lead to a lower DNA-binding affinity. However, the higher K_b value obtained suggests that the DNA-binding affinity of **1** may be due to the fact that the two ethyl groups in **1** are involved in hydrophobic interaction with the hydrophobic DNA surface leading to enhancement in DNA-binding affinity [47]. The results suggest that modification of substituents on the bridging ligands may play a vital role in DNA-binding of these copper(II) compounds. Therefore, the DNA-binding abilities of copper(II) compounds bridged both by oxamido and carboxylate groups could be regulated through varying the hydrophobicity of substituents on the bridging ligands. Indeed, further investigations on this and similar systems are still required to confirm the effect and gain deeper insights into DNA interactions.

We also compared the DNA-binding properties of **1** with those of previously reported polycopper(II) complexes with various bridging ligands and polypyridines as terminal

ligands [48–51], and we find that not only the interaction modes but also the DNA-binding ability of these polycopper(II) complexes are different, suggesting that interactions of these complexes toward DNA may be tuned by changing the bridging or terminal ligands. Such strategy should be valuable in designing new polynuclear complex systems and understanding the binding between these polynuclear complexes and DNA.

3.5.2. Fluorescence titration. To further verify the interaction mode between **1** and *HS*-DNA, EB fluorescence displacement assay was also carried out. It has been found that the intrinsic fluorescence intensity of DNA is very low and that EB in Tris–HCl buffer is also not high due to the quenching by solvent. However, EB emits intense fluorescence in the presence of DNA due to its strong intercalation between adjacent DNA base pairs. A competitive binding of metal complexes to DNA can result in reduction of the emission intensity due to decreasing of the binding sites of the DNA available for EB [45]. Thus, EB can be used to probe the interaction of metal complexes with DNA, which will provide indirect evidence for an intercalative binding mode. The extent of fluorescence quenching may also be used to determine the extent of binding between the quencher and DNA. In our experiment, as illustrated in figure 5, the fluorescence intensity of EB bound to *HS*-DNA shows a remarkable decrease at 584 nm with increasing concentration of **1**. The observed decrease in fluorescence intensity clearly indicates that some EB molecules are released from the EB-DNA system after exchange with **1**, which results in fluorescence quenching of EB. This is often considered as the characteristic of intercalation [52].

In order to understand quantitatively the magnitude of the binding strength of **1** with *HS*-DNA, the classical linear Stern–Volmer equation was employed [53]:

$$I_0/I = 1 + K_{sv}[Q] \tag{2}$$

where I_0 and I represent the fluorescence intensities in the absence and presence of quencher, respectively. K_{sv} is a linear Stern–Volmer quenching constant and $[Q]$ is the concentration of quencher. The K_{sv} value is given by the quenching plot of I_0/I *versus*

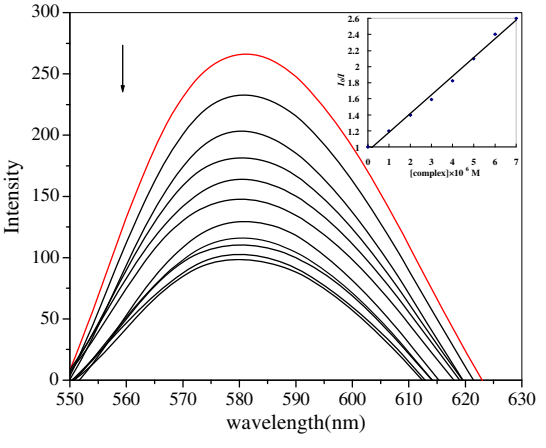

Figure 5. Emission spectra of *HS*-DNA-EB system upon titration of **1**. Arrow shows the change upon increasing concentration of **1**. Inset: plot of I_0/I *vs.* [complex] for titration of **1** to *HS*-DNA-EB system.

[complex]. As shown in the inset to figure 5, the K_{sv} value for **1** is 8.46×10^6 ($R = 0.9979$ for eight points). Therefore, based on the EB fluorescence displacement experiments, we conclude that **1** binds to *HS*-DNA through intercalation, which is in agreement with that derived by electronic absorption spectra measurements.

3.5.3. Electrochemical titration. Optical photophysical probes are necessary, but not sufficient clues to support a binding mode of metal complexes to DNA. Therefore, cyclic voltammetry was also employed to explore the nature of DNA-binding of **1**, as a complement to the previously used spectral studies. As shown in figure 6, in the absence of *HS*-DNA (red curve), **1** shows a quasi-reversible redox process corresponding to Cu(II)/Cu(I) with the cathodic (E_{pc}) and anodic peak potentials (E_{pa}) being −0.554 and −0.150 V, respectively. The separation of anodic and cathodic peaks (ΔE_p) is 0.404 V, indicating that a quasi-reversible, one-electron redox process occurred in **1**. The formal potential of the Cu (I)/Cu(II) couple ($E_f^{0\prime}$) taken as the average of E_{pc} and E_{pa} is −0.352 V. Upon addition of *HS*-DNA (blue curve) with $R = 4$ (R = [DNA]/[polymer]), the voltammetric peak current decreased, indicating that there exists interaction between **1** and *HS*-DNA [54]. The drop of the voltammetric current in the presence of *HS*-DNA may be attributed to slow diffusion of **1** bound to *HS*-DNA. The cathodic and anodic peak potentials are −0.548 and −0.132 V, respectively. The peak-to-peak separation becomes larger with $\Delta E_p = 0.416$ V, suggesting that in the presence of *HS*-DNA, the electron-transfer process seems to become less reversible for **1**. The corresponding formal potential of the Cu(I)/Cu(II) couple in binding form $E_b^{0\prime}$ (−0.340 V) is shifted positive by 0.012 V, validating that **1** could bind intercalatively to *HS*-DNA [55]. This result is in agreement with the above spectral observations. The separation between $E_b^{0\prime}$ and $E_f^{0\prime}$ can be used to estimate the ratio of binding constants for the reduced and oxidized forms to DNA using the equation as follows [55]:

$$E_b^{0\prime} - E_f^{0\prime} = 0.059 \log[K_{Cu(I)}/K_{Cu(II)}] \tag{3}$$

where $K_{Cu(I)}$ and $K_{Cu(II)}$ are the binding constants of Cu(I) and Cu(II) forms to DNA, respectively. The ratio of constants for the binding of the Cu(I) and Cu(II) ions to *HS*-DNA

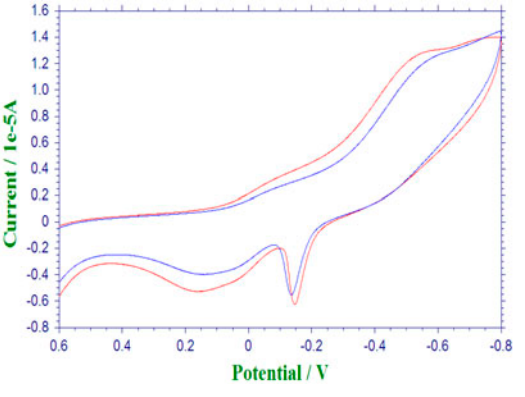

Figure 6. Cyclic voltammograms of **1** in the absence (red line) and presence (blue line) of *HS*-DNA (see http://dx.doi.org/10.1080/00958972.2015.1009452 for color version).

was estimated to be 1.60 for **1**, intimating that the reduced form of **1** interacts more strongly than the oxidized one. Thus, the electrochemical results are in agreement with the above spectral studies, further reinforcing the conclusion that **1** can bind to *HS*-DNA by intercalation.

3.5.4. Viscosity measurements. Further clarification of the interaction between **1** and *HS*-DNA is carried out by viscosity measurements. Sensitive to changes in the length of DNA molecule, viscosity measurement is regarded as the least ambiguous and most critical means of studying the binding of metal complexes with DNA in solution in the absence of crystallographic structural data, and provides reliable arguments for intercalative binding mode [27]. Generally, viscosity depends on both size and shape, and viscosity increases suggest that the DNA adopts a more open structure, due to classical intercalation. On the contrary, a partial or non-classical intercalation causes a compaction in DNA helix reducing its effective length and thereby its viscosity. The effects of **1** on the viscosity of *HS*-DNA are shown in figure 7. As illustrated in this figure, with increasing concentration of **1,** the relative viscosity of *HS*-DNA increases steadily, proving that **1** can bind to *HS*-DNA by intercalation [56]. The viscosity studies further validate those obtained from electronic absorption titration, fluorescence titration, and electrochemical titration.

These DNA studies for **1** prompt us to explore its protein binding activity.

3.6. *Protein BSA-binding activity studies*

Proteins are major targets for many types of medicines, which may influence the pharmaceutical pharmacokinetics and structure–activity relationships. Thus, it is important to understand the mechanism of interaction of a bioactive compound with proteins. The nature and magnitude of drug–protein interaction influence the biological activity of the drug [56]. It is important to study the binding parameters to control the pharmacological response of

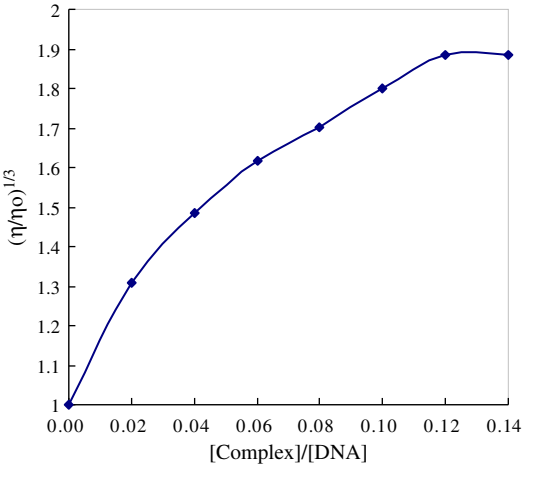

Figure 7. Effect of the increasing amount of **1** on the relative viscosity of *HS*-DNA at 289(±0.1) K, [DNA] = 0.1 mM.

drugs and design of dosage forms. Studies on binding of metal complexes with protein may provide salient information on the structural features that determine the therapeutic effectiveness of drugs and are becoming increasingly important for interpreting metabolism and transporting processes. Serum albumins, the most abundant protein in the blood circulatory system, play important roles in transport and deposition of a variety of exogenous compounds. In the present work, BSA was chosen as the model protein due to its structural homology with human serum albumin, its availability, and unusual ligand binding properties. Therefore, the BSA-binding activities of **1** were studied through tryptophan quenching and UV absorption spectral experiments.

3.6.1. Tryptophan quenching experiment. Studies related to the binding of metal complexes with BSA are usually examined by fluorescence spectroscopic techniques. BSA contains three fluorophores including tryptophan, tyrosine, and phenylalanine, while the intrinsic fluorescence of BSA is mainly attributed to tryptophan [57]. Therefore, the tryptophan fluorescence of BSA can provide structural information of the protein and it can be employed in understanding the protein folding mechanism and association reactions. There are two tryptophan residues (Trp-134 and Trp-212) in a BSA molecule. Trp-134 is located in a hydrophilic environment close to the protein surface, while Trp-212 is surrounded by a hydrophobic environment within a protein pocket. The emission intensity depends on the degree of exposure of the two tryptophan side chains, Trp-134 and Trp-212, to polar solvent [58]. Quenching can occur by different mechanisms, which are usually classified as dynamic quenching and static quenching [59]. Static quenching refers to fluorophore–quencher complex formation, while dynamic quenching refers to a process where the fluorophore and the quencher come into contact during the transient existence of the excited state [60].

To further investigate the binding activity of **1** with protein, tryptophan emission-quenching experiments were carried out using BSA in the presence of **1**. As illustrated in figure 8, the fluorescence emission intensity of BSA at 347 nm decreases with increasing

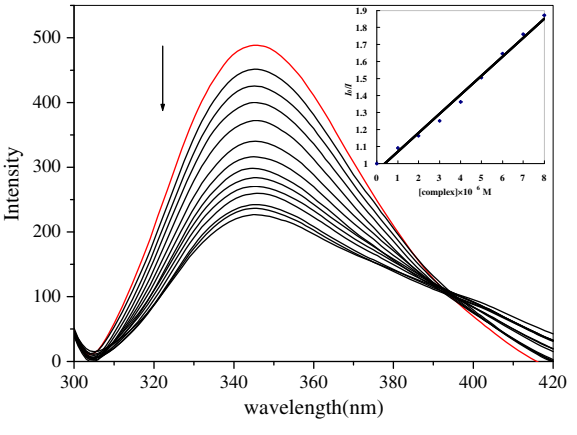

Figure 8. Emission spectra of BSA upon titration of **1**. Arrow shows the change upon increasing concentration of **1**. Inset: plot of I_0/I *vs.* [complex] for titration of **1** to BSA.

concentration of **1**, indicating that the interaction of **1** with BSA results in changes in protein secondary structure, therefore leading to changes in tryptophan environment of BSA [61]. The linear Stern–Volmer equation is also employed to understand quantitatively the ability of **1** to quench the emission intensity of BSA:

$$I_0/I = 1 + K_{sv}[Q] = 1 + K_q\tau_0[Q] \quad (4)$$

where I_0 and I represent the fluorescence intensities in the absence and presence of quencher, respectively. Q is the concentration of quencher. K_{sv} is a linear Stern–Volmer quenching constant. K_q is the biomolecular quenching rate constant and τ_0 is the average lifetime of the fluorophore in the absence of the quencher (10^{-8} s). From the quenching plot of I_0/I *versus* [complex] (inset in figure 8), K_{sv} and K_q for **1** are $1.17 \times 10^5\ M^{-1}$ and $1.2 \times 10^{13}\ M^{-1}\ s^{-1}$ ($R = 0.9951$ for nine points), respectively. Obviously, K_q of BSA quenching initiated by **1** is higher than $2.0 \times 10^{10}\ M^{-1}\ s^{-1}$, which is the maximum collision quenching constant of various kinds of quenchers to biomacromolecule [62], indicating that the above quenching is not initiated by dynamic collision but via the static quenching mechanism, and this viewpoint was also validated by the following UV absorption spectral studies.

3.6.2. UV spectral titration. UV absorption spectra help study interactions between metal complexes and plasma proteins. In general, serum albumin has been used because of its high sensitivity, rapidity, and ease of implementation [63]. To confirm the probable quenching mechanism of **1**, UV absorption spectral experiments were employed. The UV absorption spectral titrations of BSA in the presence of different concentrations of **1** are shown in figure 9. Free BSA has two absorptions, one strong absorption at 226 nm from the π–π^* transition of the characteristic polypeptide backbone structure C=O groups and the other weak absorption at 278 nm due to polarity of the microenvironment around tyrosine and tryptophan residues of BSA. From figure 9, the intensity of the absorption at 226 decreased

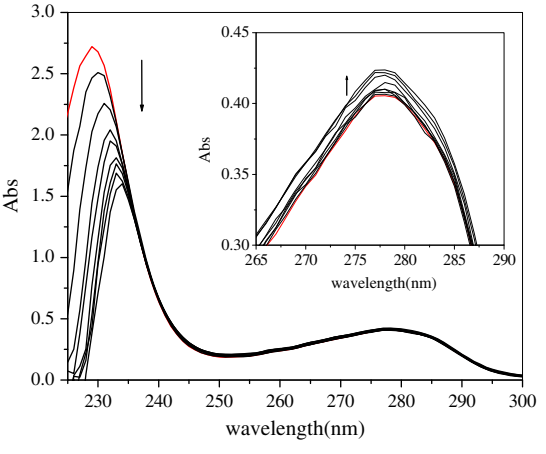

Figure 9. Absorption spectra of BSA upon titration of **1**. Arrow indicates the change upon increasing concentration of **1**.

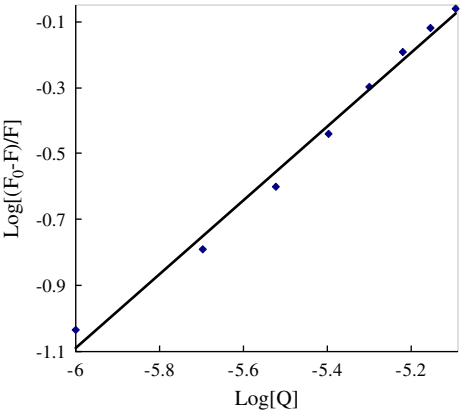

Figure 10. Plot of $\log[(F_0 - F)/F]$ *vs.* $\log[Q]$ for titration of **1** to BSA.

with addition of **1**, accompanied by red-shift of 7 nm, whereas the intensity of the peak at 278 nm increased with slight blue-shift. These results indicate that the interaction of **1** with BSA may cause conformational changes in BSA and change the polarity of the microenvironment around tyrosine and tryptophan residues of BSA [60]. Moreover, it confirms that **1** interacted with BSA to form a ground-state system, validating that the fluorescence quenching was mainly through a static quenching process [64], in agreement with the observation derived by the tryptophan emission-quenching studies.

3.6.3. Binding constant and number of binding sites. It is well documented [65, 66] that when small molecules bind independently to a set of equivalent sites on a macromolecule, the equilibrium between the free and bound molecules is given by:

$$\log[(F_0 - F)/F] = \log K + n \log[Q] \tag{5}$$

where F_0 and F represent the fluorescence intensities in the absence and presence of quencher, respectively. K is the binding constant of **1** with BSA and n is the number of binding sites. From the quenching plot of $\log[(F_0 - F)/F]$ *versus* $\log[Q]$, as illustrated in figure 10, the K and n of **1** can be obtained. The K and n values are 4.49×10^5 ($R = 0.9948$ for eight points) and 1.12, respectively. The number of binding sites n is about 1, indicating that there is just a single binding site in BSA for **1**. Considering the large size and steric effect of **1**, we believe that **1** does not rapidly penetrate the hydrophobic interior of BSA and only those tryptophan residues on the surface of the protein are quenched. Therefore, **1** most likely binds to BSA through the surface site Trp-134 [67].

In view of the premise that **1** displayed an appreciable interaction with biological macromolecules, such as DNA and protein BSA, it was pertinent to investigate the *in vitro* anticancer activity of **1**.

3.7. In vitro *antitumor activity studies*

To explore the potential antitumor activities of **1**, cytotoxicity assays of **1** and cisplatin against human hepatocellular carcinoma SMMC-7721 and human lung adenocarcinoma

A549 were conducted. The IC_{50} values 9.2 ± 0.4 and 10.5 ± 0.9 μM for SMMC-7721 and A549, respectively, indicate that **1** demonstrated anticancer activities. This may be partially attributed to its strong intercalation. Furthermore, the IC_{50} values of **1** are higher than those of cisplatin (IC_{50} values are 5.4 ± 0.2 and 7.6 ± 0.4 μM to these two kinds of cancer cell lines, respectively), suggesting that the cytotoxic activities of **1** are less than that of cisplatin. However, the inhibition of cell proliferation produced by **1** on the same batch of cell lines is significant. The hydroxo-bridged oligomeric and polymeric species (the hydrolyzed product *in vivo*) of platinum complexes are toxic to the body and such polymeric species may have lower water solubility. These two factors may be incorporated in the list of drugs, which should be further studied in order to obtain some insights into the anticancer mechanism of this kind of polymer–metal systems.

Comparing the IC_{50} values of **1** with those of our previously reported analogous copper (II) compounds $\{[Cu_2(dmaepox)(dabt)](pic)\cdot H_2O\}_n$ and $\{[Cu_2(dmapob)(dabt)](NO_3)\cdot 0.6H_2O\}_n$, we found that **1** possessed the lowest IC_{50} values for the same cancer cell lines among the three copper(II) compounds [20], indicating that **1** has the most potent inhibitory effect against the two selected cancer cell lines under identical experimental conditions. This may be due to the enhanced hydrophobicity of the two methyl groups on the bridging ligand in **1**, which may favor the permeation through the lipid layers of the cell membrane. Thus, according to these results, we conclude that the hydrophobic interaction of the ethyl groups on the bridging ligand in **1** may be the major cause of the enhanced activity. The order of the *in vitro* anticancer activities of the three copper(II) compounds against the selected cancer cell lines is in accord with their DNA-binding abilities, implying that the *in vitro* anticancer activities of these copper(II) compounds may be closely related to or originate from their ability to intercalate the base pairs of DNA. Thus, these copper(II) compounds might target DNA, leading to cell death. This fact indicates that the DNA-binding and the *in vitro* anticancer activities could possibly be tuned through varying the hydrophobicity of the substituents on bridging ligands in these polymeric copper(II) compounds. This strategy offers perspectives in understanding the anticancer activities and DNA-binding behaviors of this kind of copper(II) compounds, providing information on the mechanism of anticancer drugs binding to DNA and thus will be beneficial to new drug design.

4. Conclusion

To investigate the influence of hydrophobic interaction of different substituents on bridging ligands in polymeric copper(II) complexes on DNA/BSA binding properties and *in vitro* anticancer activities, and also gain insight into structure–activity relationships of polymeric copper(II) systems, our article describes the synthesis and structural characterization of a copper(II) polymer bridged by oxamide and carboxylate groups, $\{[Cu_2(bdpox)(dabt)](NO_3)\cdot H_2O\}_n$. The DNA and protein BSA binding properties as well as *in vitro* anticancer activities of the polymeric copper(II) complex are investigated and compared with other polycopper(II) complexes. Reactivity toward *HS*-DNA and BSA reveals that **1** interacts with *HS*-DNA by intercalation and to BSA through quenching of tryptophan fluorescence by static quenching mechanism. The *in vitro* cytotoxic activities suggest that **1** is active against selected tumor cell lines. Comparing the DNA-binding properties and *in vitro* anticancer activities with our previously reported polymeric copper(II) complexes with different bridging ligands [20], the different substituents on bridging ligands in these polymeric

copper(II) complexes result in differences in the space configuration and electron density distribution, thus changing the DNA-binding abilities and *in vitro* anticancer activities through varying the hydrophobicity. The *in vitro* anticancer activities of these polymeric copper(II) complexes are in accord with their DNA-binding abilities. These results imply that the anticancer activities of these polymeric copper(II) complexes may be associated with their ability to intercalate the base pairs of DNA. The DNA-binding abilities and *in vitro* anticancer activities could be tuned through changing the hydrophobicity of bridging ligands in these polymeric copper(II) complexes. Such strategy should be valuable for understanding the mechanism of anticancer drugs binding to DNA, and for laying a foundation for the rational design of highly effective agents for probing and targeting nucleic acids and proteins.

Supplementary material

CCDC 917219 contains the supplementary crystallographic data for this article. Copies of this information can be obtained for free from the Director, CCDC, 12 Union Road, Cambridge, CB2 1EZ, UK (Fax: C44 1233 336 033; E-mail: deposit@ccdc.cam.ac.uk).

Funding

This project was supported by the National Natural Science Foundation of China [grant number 51273184], [grant number 81202399]; the Program for Science and Technology of Shandong Province [grant number 2011GHY11521]; the key laboratory open funds of marine biological active substances and modern analytical technology of the state oceanic administration [MBSMAT-2012-05]; the Natural Science Foundation of Qingdao City [grant number 12-1-3-52-(1)-nsh], [grant number 12-1-4-16-(7)-jch].

References

[1] S.R. Dalton, S. Glazier, B. Leung, S. Win, C. Megatulski, S.J.N. Burgmayer. *J. Biol. Inorg. Chem.*, **13**, 1133 (2008).
[2] S. Ray, R. Mohan, J.K. Singh, M.K. Samantaray, M.M. Shaikh, D. Panda, P. Ghosh. *J. Am. Chem. Soc.*, **129**, 15042 (2007).
[3] E. Meggers. *Angew. Chem. Int. Ed.*, **50**, 2442 (2011).
[4] G. Sava, G. Jaouen, E.A. Hillard, A. Bergamo. *Dalton Trans.*, **41**, 8226 (2012).
[5] C.G. Hartinger, N. Metzler-Nolte, P.J. Dyson. *Organometallics*, **31**, 5677 (2012).
[6] N.P. Barry, P.J. Sadler. *Chem. Commun.*, **49**, 5106 (2013).
[7] D.R. Green, J.C. Reed. *Science*, **281**, 1309 (1998).
[8] S. Dhar, M. Nethaji, A.R. Chakravarty. *Inorg. Chim. Acta*, **358**, 2437 (2005).
[9] A.M. Thomas, M. Nethaji, A.R. Chakravarty. *J. Inorg. Biochem.*, **98**, 1087 (2004).
[10] M. Jiang, Y.T. Li, Z.Y. Wu, Z.Q. Liu, C.W. Yan. *J. Inorg. Biochem.*, **103**, 833 (2009).
[11] A.M. Thomas, G. Neelakanta, S. Mahadevan, M. Nethaji, A.R. Chakravarty. *Eur. J. Inorg. Chem.*, **2002**, 2720 (2002).
[12] R. Kumar, S. Arunachalam. *Polyhedron*, **25**, 3113 (2006).
[13] S.K. Rajendran, A. Sankaralingam. *Eur. J. Med. Chem.*, **44**, 1878 (2009).
[14] E. Dfaz, R. Valenciano, P. Landa, J.L. Arana, J. Gonzalez. *Polym. Test.*, **21**, 247 (2002).
[15] I.A. Katime, J.R. Ochoa, C. Nido. *J. Appl. Polym. Sci.*, **34**, 1953 (1987).
[16] B. Schechter, R. Arnon, M. Wilchek. *React. Polym.*, **25**, 167 (1995).
[17] H. Sasaki. *Tetrahedron Lett.*, **35**, 4401 (1994).
[18] L.M. Fisher, R. Kuroda, T.T. Sakai. *Biochemistry*, **24**, 3199 (1985).
[19] M.J. Waring. *Annu. Rev. Biochem.*, **50**, 159 (1981).
[20] L.L. Zhang, L.D. Wang, Y.T. Li, Z.Y. Wu, C.W. Yan. *J. Inorg. Organomet. Polym. Mater.*, **22**, 1128 (2012).
[21] J.J. Nie, Y.T. Li, Z.Y. Wu, X.W. Li, C.W. Yan. *Acta Cryst.*, **C66**, 327 (2010).

[22] H. Ojima, K. Yamada. *Bull. Chem. Soc. Jpn.*, **43**, 3018 (1970).
[23] G.M. Sheldrick. *SHELXL97, Program for Crystal Structure Refinement*, University of Göttingen, Göttingen (1997).
[24] J. Marmur. *J. Mol. Biol.*, **3**, 208 (1961).
[25] M.E. Reichmann, S.A. Rice, C.A. Thomas, P.J. Doty. *J. Am. Chem. Soc.*, **76**, 3047 (1954).
[26] J.B. Chaires, N. Dattagupta, D.M. Crothers. *Biochemistry*, **21**, 3933 (1982).
[27] S. Satyanarayana, J.C. Dabrowiak, J.B. Chaires. *Biochemistry*, **31**, 9319 (1992).
[28] J.K. Barton, J.M. Goldberg, C.V. Kumar, N.J. Turro. *J. Am. Chem. Soc.*, **108**, 2081 (1986).
[29] N.S. Quiming, R.B. Vergel, M.G. Nicolas, J.A. Villanueva. *J. Health Sci.*, **51**, 8 (2005).
[30] K. Nakamoto. *Infrared and Raman Spectra of Inorganic and Coordination Compounds*, 5th Edn, Wiley, New York, NY (1997).
[31] A.B.P. Lever. *Inorganic Electronic Spectroscopy*, Elsevier Science Publishers BV, Amsterdam (1984).
[32] A.W. Addison, T.N. Rao, J. Reedijk, J. van Rijn, G.C. Verschoor. *J. Chem. Soc., Dalton Trans.*, 1349 (1984).
[33] Y.X. Tong, X.M. Chen, S. Weng Ng. *Polyhedron*, **16**, 3363 (1997).
[34] L.M. Duan, F.T. Xie, X.Y. Chen, Y. Chen, Y.K. Lu, P. Cheng, J.Q. Xu. *Cryst. Growth Des.*, **6**, 1101 (2006).
[35] D. Cremer, J.A. Pople. *J. Am. Chem. Soc.*, **97**, 1354 (1975).
[36] M. Baldini, M. Belicchi-Ferrari, F. Bisceglie, P.P. Dall'Aglio, G. Pelosi, S. Pinelli, P. Tarasconi. *Inorg. Chem.*, **43**, 7170 (2004).
[37] W.J. Geary. *Coord. Chem. Rev.*, **7**, 81 (1971).
[38] S. Mahadevan, M. Palaniandavar. *Inorg. Chem.*, **37**, 693 (1998).
[39] S.E. Evans, M.A. Mendez, K.B. Turner, L.R. Keating, R.T. Grimes, S. Melchoir, V.A. Szalai. *J. Biol. Inorg. Chem.*, **12**, 1235 (2007).
[40] M. Sunita, M. Padmaja, B. Anupama, C. Kumari. *J. Fluoresc.*, **22**, 1003 (2012).
[41] T. Gupta, S. Dhar, M. Nethaji, A.R. Chakravarty. *Dalton Trans.*, 1896 (2004).
[42] X.W. Li, Y.T. Li, Z.Y. Wu, C.W. Yan. *Inorg. Chim. Acta*, **390**, 190 (2012).
[43] M. Iqbal, S. Ali, Z.U. Rehman, N. Muhammad, M. Sohail, V. Pandarinathan. *J. Coord. Chem.*, **67**, 1731 (2014).
[44] R.K.B. Devi, S.P. Devi, R.K.B. Singh, R.K.H. Singh, T. Swu, W.R. Devi, C.B. Singh. *J. Coord. Chem.*, **67**, 891 (2014).
[45] X. Li, X.J. Li, Y.T. Li, Z.Y. Wu, C.W. Yan. *New J. Chem.*, **36**, 2472 (2012).
[46] S. Sharma, S.K. Singh, M. Chandra, D.S. Pandey. *J. Inorg. Biochem.*, **99**, 458 (2005).
[47] V. Rajendiran, R. Karthik, M. Palaniandavar, H. Stoeckli-Evans, V.S. Periasamy, M.A. Akbarsha, B.S. Srinag, H. Krishnamurthy. *Inorg. Chem.*, **46**, 8208 (2007).
[48] S. Anbu, A. Killivalavan, E.C.B.A. Alegria, G. Mathan, M. Kandaswamy. *J. Coord. Chem.*, **66**, 3989 (2013).
[49] J. Lu, J.L. Li, Q. Sun, L. Jiang, B.W. Wang, W. Gu, X. Liu, J.L. Tian, S.P. Yan. *J. Coord. Chem.*, **67**, 300 (2014).
[50] X.L. Wang, M. Jiang, Y.T. Li, Z.-Y. Wu, C.W. Yan. *J. Coord. Chem.*, **66**, 1985 (2013).
[51] T.T. Xing, S.H. Zhan, Y.T. Li, Z.Y. Wu, C.W. Yan. *J. Coord. Chem.*, **66**, 3149 (2013).
[52] O. Stern, M. Volmer. *Z. Phys.*, **20**, 183 (1919).
[53] X.W. Li, Y.J. Zheng, Y.T. Li, Z.Y. Wu, C.W. Yan. *Eur. J. Med. Chem.*, **46**, 3851 (2011).
[54] Y.M. Song, P.J. Yang, M.L. Yang, J.W. Kang, S.Q. Qin, B.Q. Lü. *Transition Met. Chem.*, **28**, 712 (2003).
[55] M.T. Carter, M. Rodriguez, A.J. Bard. *J. Am. Chem. Soc.*, **111**, 8901 (1989).
[56] H. Malonga, J.F. Neault, H.A. Tajmir-Riahi. *DNA Cell Biol.*, **25**, 393 (2006).
[57] A.S. Kowska. *J. Mol. Struct.*, **614**, 227 (2002).
[58] T. Peters. *Adv. Protein Chem.*, **37**, 161 (1985).
[59] A. Papadopoulou, R.J. Green, R.A. Frazier. *J. Agric. Food Chem.*, **53**, 158 (2005).
[60] G. Vignesh, S. Arunachalam, S. Vignesh, R.A. James. *Spectrochim. Acta, Part A*, **96**, 108 (2012).
[61] S.S. Bhat, A.A. Kumbhar, H. Heptullah, A.A. Khan, V.V. Gobre, S.P. Gejji, V.G. Puranik. *Inorg. Chem.*, **50**, 545 (2011).
[62] W.R. Ware. *J. Phys. Chem.*, **66**, 455 (1962).
[63] S. Ashoka, J. Seetharamappa, P.B. Kandagal, S.M.T. Shaikh. *J. Lumin.*, **121**, 179 (2006).
[64] D. Senthil Raja, N.S.P. Bhuvanesh, K. Natarajan. *Eur. J. Med. Chem.*, **47**, 73 (2012).
[65] V. Anbazhagan, R. Renganathan. *J. Lumin.*, **128**, 1454 (2008).
[66] P. Banerjee, S. Ghosh, A. Sarkar, S.C. Bhattacharya. *J. Lumin.*, **131**, 316 (2011).
[67] F. Xue, C.Z. Xie, Y.W. Zhang, Z. Qiao, X. Qiao, J.Y. Xu, S.P. Yan. *J. Inorg. Biochem.*, **115**, 78 (2012).